Proceedings of the 28th IEEE
EMBS Annual International Conference
New York City, USA, Aug 30-Sept 3, 2006

Effect of Ultrasound Probe on Dose Delivery During Real-time Ultrasound-Guided Tumor Tracking

Jianzhou Wu, Omkar Dandekar, Daryl Nazareth, Peng Lei, Warren D'Souza, and Raj Shekhar

Abstract—**Ultrasound is a noninvasive and less costly modality for real-time imaging of soft tissues. It has the capability of tracking soft tissue at levels of submillimeter precision even in the presence of radiation beams. The effect of a transducer on radiation dose is not fully known. The best imaging location for an ultrasound transducer happens to coincide with the path of an anterior–posterior beam in intensity modulated radiation therapy (IMRT). This study indicates a significant change in dose when this juxtaposition occurs. If the anterior–posterior beam is avoided in IMRT planning, however, the effect of the transducer on radiotherapy is found to be negligible.**

I. INTRODUCTION

The goal of radiation therapy is to deliver a lethal dose precisely to the tumor while minimizing the dose to surrounding healthy tissues and critical structures. Recent technical developments, such as three-dimensional (3D) conformal radiation therapy and 3D intensity-modulated radiation therapy (IMRT), are capable of realizing such a goal. However, these techniques are quite sensitive to set-up uncertainties, interfraction tumor shifts and deformation, and intrafraction tumor motion [1–3]. Tumors in the lung, pancreas, and other thoracic and abdominal regions are susceptible to internal organ motion. When applying IMRT to these tumors, tumor periphery is likely to be underdosed as a result of motion.

To deliver the prescribed radiation dose to the entire volume of moving tumors, the conventional approach is to create a planning target volume (PTV) by adding a margin around the clinical target volume (CTV). This margin should be sufficiently large to accommodate the motion of CTV within the PTV. The high dose treatment is planned for the PTV rather than the CTV. By adding an appropriate margin to compensate for internal target motion and set-up uncertainties, the tumor periphery receives a higher dose. This approach, however, increases the risk that healthy tissues and critical structures surrounding the tumor will receive significant radiation. Therefore, treatment based on PTV is the least desirable option. Another way to deliver the prescribed dose to the tumor periphery is to minimize tumor motion. For example, breath holding or gating is used to reduce respiration-induced target motion, rectal balloons are used to minimize prostate motion [4–6], etc. Breath holding and gating minimize tumor motion, but are achieved with the trade-off of dramatically extended treatment times. Moreover, this approach minimizes but does not remove target motion.

The most promising way to deliver radiation on a moving target is under real-time tumor tracking, an approach that is still under development. With real-time tracking information, one can compensate for tumor motion by letting the radiation beam follow the tumor dynamically [7] or by moving the couch the same distance the tumor moves, (although in the opposite direction [8]). Tumor location can be either directly or indirectly inferred. In the direct manner, mental markers are implanted into or near the patient's tumor and fluoroscopic kV X-rays are used to trace the marker location directly [9]. In the indirect manner, plastic markers are placed on the patient's body and the reflected laser signals of these markers are collected to deduce the spatial location of the tumor [10]. Tracking the implanted mental markers provides a highly effective way for real-time tumor monitoring. However, fluoroscopy exposes patients to high skin doses. The implantation process may cause additional patient suffering and increase the potential for infection. Tracking tumor motion by using external markers avoids these disadvantages but is susceptible to the daily variations in correlation between the motion of the external markers and that of the tumor.

Other ways to monitor a target involve computed tomography (CT) and magnetic resonance (MR) imaging [11]. Continuous imaging with either CT or MR during treatment delivery poses a number of significant difficulties. Ultrasound, on the other hand, is a perfect modality for real-time imaging of soft tissue, such as the prostate. With the recent development of ultrasound imaging of soft tissues [12], ultrasound has attracted substantial scientific interest for its potential application in real-time tumor tracking during treatment delivery [13]. Hsu et al. demonstrated that ultrasound has the capability to track soft tissue to submillimeter precision even in the presence of radiation beams [14]. We report here on changes to the prescribed dose when the ultrasound probe intersects the radiation beams in the context of IMRT of prostate tumors.

Manuscript received April 3, 2006. This work was supported in part by Department of Defense grant DAMD17-99-1-9034.

Jianzhou Wu is with the Departments of Radiation Oncology and Diagnostic Radiology, University of Maryland School of Medicine, Baltimore, MD 21201 USA (e-mail: jwu@umm.edu).

Omkar Dandekar is with the Department of Diagnostic Radiology, University of Maryland School of Medicine, Baltimore, MD 21201 USA.

Daryl Nazareth is with the Department of Radiation Oncology, University of Maryland School of Medicine, Baltimore, MD 21201 USA.

Peng Lei is with the Department of Diagnostic Radiology, University of Maryland School of Medicine, Baltimore, MD 21201 USA.

Warren D'Souza is with the Department of Radiation Oncology, University of Maryland School of Medicine, Baltimore, MD 21201 USA.

Raj Shekhar, the corresponding author, is with the Department of Diagnostic Radiology, University of Maryland School of Medicine, Baltimore, MD 21201 USA. (phone: 410-706-8714; fax: 410-706-8724; e-mail: rshekhar@umm.edu).

1-4244-0033-3/06/$20.00 ©2006 IEEE.

II. MATERIALS AND METHODS

Patients and an ultrasound probe were scanned using a helical CT scanner. A synthetic CT image was created by superimposing the probe image on the patient's CT image. IMRT planning was first performed on the patient's CT image. The treatment plan was then copied onto the synthetic CT image and the dose recalculated. The treatment isocenter remained invariant in the room coordinate system. The effect of the transducer on radiotherapy was studied by comparing the two dose distributions.

A. Image Acquisition

Sequential CT scans of patients with prostate cancer were acquired on a spiral PQ 5000 scanner (Philips Medical Systems, Cleveland, OH). An Acuson 4C1 ultrasound transducer probe (Siemens Medical Solutions USA, Mountain View, CA) was also scanned. A synthetic CT image was generated by adding the Acuson 4C1 probe image to the patient's image, as if the CT scan of the patient was taken with the ultrasound probe in the field of view. The volume of the transducer is the most important factor in studying the effect on radiotherapy, and the Acuson 4C1 was chosen for image synthesis because its volume is comparable with and consonant to those models most likely to be used in real-time target monitoring.

B. Synthetic Image

The optimal approach to imaging the prostate is to place the ultrasound probe directly above the prostate on the abdomen while the patient is supine on the treatment couch. This location, however, interferes with the entering anterior–posterior radiation and represents the worst-case scenario for dose change. To study the dose change in such a situation, where the anterior–posterior beam is attenuated, we first performed IMRT planning with one of the beams in the anterior–posterior direction. Next, we synthesized CT images by aligning the axis of the transducer in the anterior–posterior direction. This was performed by manual rigid registration. After alignment, the probe image was shifted around so that the axis of the transducer passed through the center of mass of the prostate and the transducer surface touched the patient's abdomen. The probe image was contoured and resampled. Voxel intensities were kept unchanged inside this contour; outside the contour, voxel intensity was set to zero. The synthetic CT image was created by adding together the patient's image and the aligned and resampled probe image. Figure 1 shows the CT image of a representative patient and the synthetic CT image.

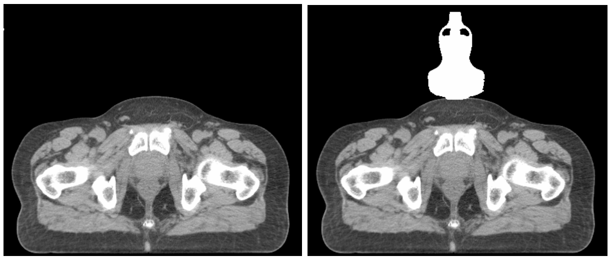

Fig. 1. Image of a representative patient (left) and the synthetic CT image (right), achieved by superimposing the image of a 2D ultrasound probe on the patient's CT image.

C. IMRT Planning

IMRT planning was performed using the Pinnacle treatment planning system (Philips Medical Systems, Madison, WI). The prescribed dose was 75.6 Gy with 180 cGy per fraction for a total 42 fractions. The patient was irradiated by seven equally spaced beams, with one beam in the anterior–posterior direction. Constraints were added before dose optimization. The planning target volume (PTV), created by adding 1 cm margin to the prostate, should receive uniform dose 75.6 Gy. For the rectum, no more than 20% of its volume should receive 60 Gy and no more than 40% of its volume receive 20 Gy. For the bladder, no more than 15% of its volume should receive 75.6 Gy, and no more than 50% of its volume receive 20 Gy. The optimization was performed with 50 iterations. The optimized plan parameters were then applied to the synthetic image. Dose was recalculated for each beam. The dose of the IMRT treatment planned on the patient's image and the dose recalculated on the synthetic image were compared.

To study the possibility of avoiding radiation beam blocking by the transducer, a second IRMT treatment planning was performed on the patient's CT image. In this plan, a posterior–anterior beam instead of an anterior–posterior beam was used. The seven beams were equally spaced. The optimized plan parameters were applied to the synthetic image and recalculated the dose for each beam.

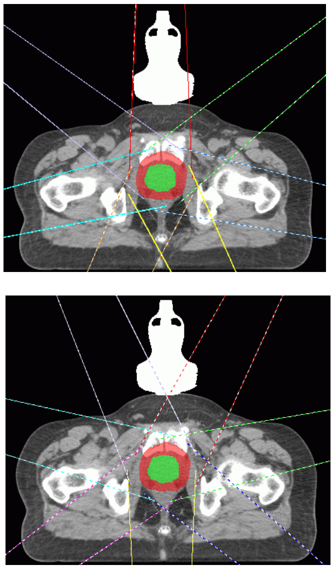

Fig. 2. Demonstration of IMRT plans copied to the synthetic images. IMRT treatment plans were performed on the patient's CT image. Plan parameters were then applied to the synthetic image, the dose was recalculated. The green-shaded region is the prostate, the red region is the PTV for treatment planning. (Top) An IMRT plan with an anterior–posterior beam was copied to the synthetic image. (Bottom) An IMRT plan with a posterior–anterior beam instead of an anterior–posterior beam was copied to the synthetic image.

Figure 2 demonstrates the application of the IMRT treatment beams to the synthetic image.

III. RESULTS

A. *Treatment Plan Using an Anterior–Posterior Beam*

An IMRT plan with one beam in the anterior–posterior direction was performed on the patient CT image. The plan parameters were then applied to the synthetic image, as shown in Figure 2(top), and the dose was calculated again. The dose-volume histograms (DVH) of the two dose distributions for the prostate were demonstrated in Figure 3. Following the IMRT treatment plan, 99% of the prostate receives at least the prescribed dose (75.6 Gy). However, the dose reduces to 71.2 Gy if a transducer is placed in the path of the anterior–posterior beam. In such a case, only 13.7% of the prostate would receive at least the prescribed dose. The mean prostate dose reduces from the planned 77.8 Gy to 73.4 Gy when the transducer blocks one of the beams. The 100% isodose curve (75.6 Gy) shrinks dramatically, as can be seen in Figure 4, where the 100% isodose curves (red and blue) and the contour of the prostate (black) are shown. The DVHs of the rectum and bladder are shown in Figure 5. The effect of the transducer on the dose distributions of these critical structures is small.

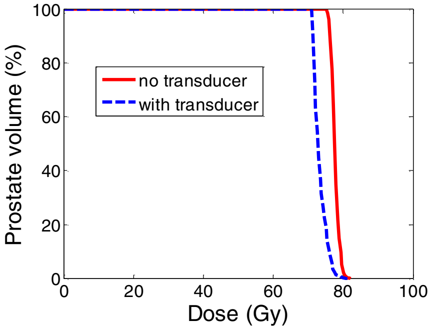

Fig. 3. Dose-volume histograms of the prostate. The red solid curve represents the DVH of the IMRT treatment planned on the patient CT image. The IMRT parameters were applied to the synthetic image, and the dose was recalculated. The blue dashed curve represents the DVH of the dose recalculated.

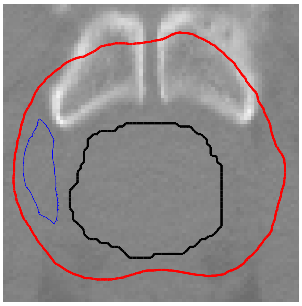

Fig. 4. The 100% isodose curves (outer red and middle blue) and the contour of the prostate (inner black). The red line is the 75.6 Gy isodose curve of the IMRT treatment planned on the patient's image. The thin blue line is the 75.6 Gy isodose curve of the dose recalculated on the synthetic image. Dramatic shrinking of the 100% isodose curve is obvious, which leads to underdosing of the prostate.

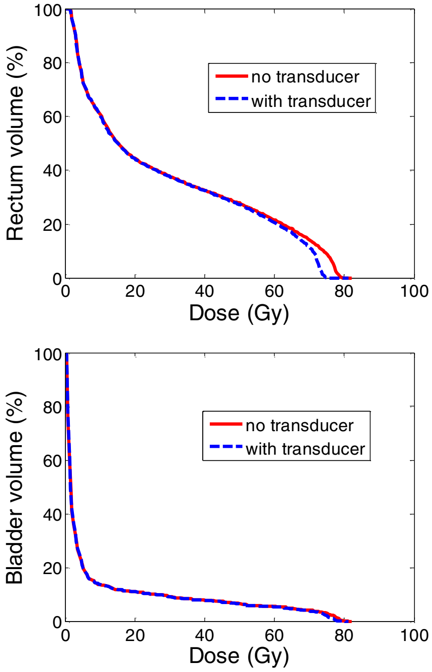

Fig. 5. Dose-volume histograms of the rectum and bladder. The red solid curves represent the DVH of the IMRT treatment planned on the patient's image. The blue dashed curves are of the dose recalculated on the synthetic image.

B. *Treatment Plan Using a Posterior–Anterior Beam*

The transducer, then, significantly alters the dose distribution when placed in the path of an anterior–posterior beam. To eliminate this effect, an IMRT plan without the anterior–posterior beam was performed with the same prescription and constraints. The same procedure as that used in the previous subsection was repeated to recalculate the dose on the synthetic image, as shown in Figure 2(bottom). The DVHs of the IMRT dose distribution and the recalculated dose distribution for the prostate are plotted in Fig. 6. The difference between the two curves is not noticeable. In this IMRT plan, 99.2% of the prostate would

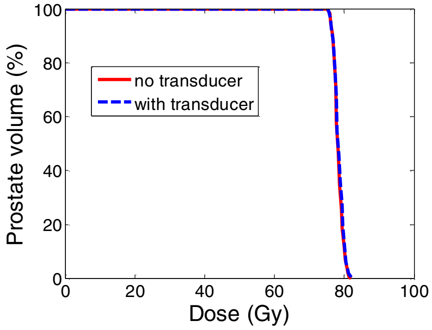

Fig. 6. Dose-volume histogram of the prostate. The solid red curve is of an IMRT treatment plan using a posterior–anterior beam instead of an anterior–posterior beam. The blue dashed curve is of the dose recalculated on the synthetic image.

receive the prescribed dose (75.6 Gy). In the recalculated dose distribution, this ratio did not change. The mean prostate dose is 78.3 Gy in the IMRT plan and 78.5 Gy in the recalculated dose distribution. None of the radiation beam is blocked or attenuated by the transducer, so that these very similar figures are to be expected. The DVHs of the rectum and bladder are shown in Figure 7.

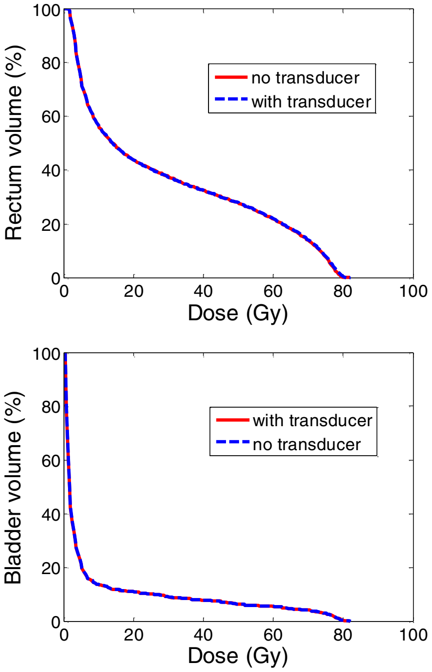

Fig. 7. Dose-volume histograms of the rectum and bladder. The solid red curves represent an IMRT treatment plan using a posterior–anterior beam. The blue dashed curves represent the recalculated dose.

IV. DISCUSSION

We studied the effect of the ultrasound transducer on radiation dose in IMRT when the transducer is placed in the path of a radiation beam. The worst scenario, in which the transducer is position at the entryway of a beam, results in significant shrinkage of the 100% isodose curve. Such an approach, involving blocking of radiation beams, would result in significant underdosing. The optimal location for ultrasound imaging of the prostate (although this may vary slightly among patients) coincides with the path of an anterior–posterior therapy beam. To eliminate the possibility of tumor underdosing, it is better to formulate an IMRT plan that does not use an anterior–posterior beam. If, however, the anterior–posterior beam cannot be avoided, the IMRT plan should be performed on the patient's image with an ultrasound probe in the field of view. In this way, the attenuation of the beam caused by the transducer can be compensated.

Ultrasound has the capability to track soft tissue with high precision, even in the presence of radiation beams—a functionality not easily offered by any other modality. This study shows that the transducer attenuates the dose distribution dramatically. However, this attenuation can be compensated by performing an IMRT plan without using an anterior–posterior beam.

V. CONCLUSION

This work indicates that the placement of an ultrasound transducer attenuates radiation dose distribution significantly when placed in the path of a radiation beam. To compensate for this attenuation, an IMRT plan without an anterior–posterior should be performed. The transducer then would have a negligible effect on dose distribution.

REFERENCES

[1] C. X. Yu, D. A. Jaffray, and J. W. Wong, "The effects of intra-fraction organ motion on the delivery of dynamic intensity modulation," *Phys. Med. Biol.* vol. 43, pp. 91–104, Jan. 1998.

[2] T. Bortfeld, K. Jokivarsi, M. Goitein, J. Kung, and S. B. Jiang, "Effects of intra-fractionmotion on IMRT dose delivery: statistical analysis and simulation" *Phys. Med. Biol.*, vol. 47, pp. 2203–2220, Jul. 2002.

[3] S. A. Naqvi and W. D. D'Souza, "Astochastic convolution / superposition method with isocenter sampling to evaluate intrafraction motion effects in IMRT," *Med. Phys.*, vol. 32. pp. 1156–1163, Apr. 2005.

[4] S. S. Vedam, P. J. Keall, V. R. Kini, and R. Mohan, "Determining parameters for respiration-gated radiotherapy," *Med. Phys.*, vol. 28, pp. 2139–2146, Oct. 2001.

[5] G. D. Hugo, N. Agazaryan, and T. D. Solberg, "An evaluation of gating window size, delivery method, and composite field dosimetry of respiratory-gated IMRT," *Med. Phys.*, vol. 29, Nov. 2002.

[6] V. M. Remouchamps, N. Letts, D. Yan, F. A. Vicini, M. Moreau, J. A. Zielinski, J. Liang, L. L. Kestin, A. A. Martinez, and J. W. Wong, "Threedimensional evaluation of intra- and interfraction immobilization of lung and chest wall using active breathing control: A reproducibility study with breast cancer patients," *Int. J. Radiat. Oncol., Biol., Phys.*, vol. 57, pp. 968–978, Nov. 2003.

[7] P. J. Keall, V. R. Kini, S. S. Vedam, and R. Mohan, "Motion adaptive x-ray therapy: a feasibility study," *Phys. Med. Biol.*, vol. 46, pp. 1–10, Jan. 2001.

[8] W. D. D'Souza, S. A. Naqvi, and C. X. Yu, "Real-time intra-fraction-motion tracking using the treatment couch: a feasibility study," *Phys. Med. Biol.*, vol. 50, pp. 4021–4033, Sept. 2005.

[9] S. Shimizu, H. Shirato, S. Ogura, H. Akita-Dosaka, K. Kitamura, T. Nishioka, K. Kagei, M. Nishimura, and K. Miyasaka, "Detection of lung tumor movement in real-time tumor-tracking radiotherapy," *Int. J. Radiat. Oncol., Biol., Phys.*, vol. 51, pp. 304–310, Oct. 2001.

[10] R. I. Berbeco, S. Nishioka, H. Shirato, G. T. Y. Chen, and S. B. Jiang, "Residual motion of lung tumors in gated radiotherapy with external respiratory surrogates," *Phys. Med. Biol.*, vol. 50, pp. 3655–3667, Aug. 2005.

[11] D. A. Jaffray, J. H. Siewerdsen, J. W. Wong, and A. A. Martinez, "Flatpanel cone-beam computed tomography for image-guided radiation therapy," *Int. J. Radiat. Oncol., Biol., Phys.*, vol. 53, pp. 1337–1349, Aug. 2002.

[12] A. Pesavento, A. Lorenz, S. Siebers and H. Ermert, "New real-time strain imaging concepts using diagnostic ultrasound," *Phys. Med. Biol.*, vol. 45, pp. 1423–1435, Jun. 2000.

[13] S. L. Meeks, J. M. Buatti, L. G. Bouchet, F. J. Bova, T. C. Ryken, E. C. Pennington, K. M. Anderson, and W. A. Friedman, "Ultrasound-guided extracranial radiosurgery: technique and application," *Int. J. Radiat. Oncol. Biol. Phys.*, vol. 55, pp. 1092–1101, Mar. 2003.

[14] A. Hsu, N. R. Miller, P. M. Evans, J. C. Bamber, and S. Webb, "Feasibility of using ultrasound for real-time tracking during radiotherapy," *Med. Phys.*, vol. 32, pp. 1500–1512, Jun. 2005.